

# *In situ* EPR investigation of the addition of persistent benzyl radicals to acrylates on ZSM-5 zeolites. Direct spectroscopic detection of the initial steps in a supramolecular photopolymerization †

Xue-gong Lei,<sup>a</sup> Steffen Jockusch,<sup>a</sup> M. Francesca Ottaviani<sup>b</sup> and Nicholas J. Turro<sup>\*a</sup>

<sup>a</sup> Department of Chemistry, Columbia University, 3000 Broadway, New York, NY 10027, USA

<sup>b</sup> Institute of Chemical Sciences, University of Urbino, Piazza Rinascimento 6, 61029 Urbino, Italy

Received 8th July 2003, Accepted 12th August 2003

First published as an Advance Article on the web 27th August 2003

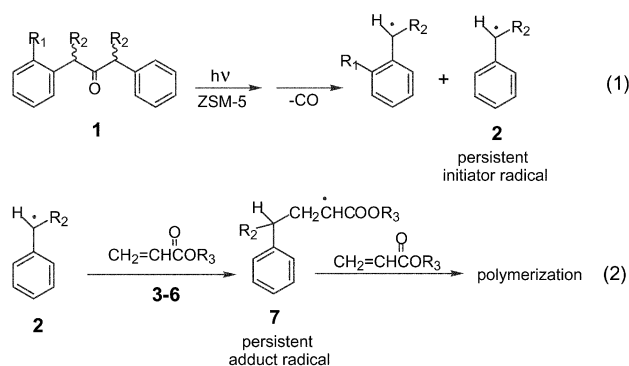
Photolysis of dibenzyl ketone derivatives adsorbed on ZSM-5 zeolites produces persistent benzyl radicals (initiator radicals), which add to methyl acrylates (monomers) to generate persistent adduct radicals. Both initiator and adduct radicals are readily observable by conventional steady-state EPR spectroscopy at room temperature and are persistent for time periods ranging from seconds to many days. The rate of the formation and the amount of the adduct persistent radical formed depends on the structure of the initiator radical (benzyl radical derivative) and the structure of the monomer (acrylate derivative). The lifetimes of the initiator and adduct radicals depend on the supramolecular structure of the radical@zeolite complex and the diffusion and reaction dynamics of the radicals in the complex. The most intense signal and highest addition rate to methyl acrylate were observed for the smallest initiator radical, the benzyl radical, because of its high mobility and relatively rapid diffusion within the internal zeolite surface. With increasing length of an alkyl chain (methyl, ethyl, and pentyl) on either the initiator ( $\alpha$  position of the radical) or monomer (alkyl group of acrylate ester), the rate of radical addition to the monomer decreased, a result that is consistent with the decreased mobility and diffusion of the initiator radical or monomer. Deuterium isotope experiments and variation of the methyl acrylate concentration demonstrated that the initial adduct radical from methyl acrylate adds to another methyl acrylate to generate a secondary adduct radical, which, in turn, can continue to propagate to form a polymer that is cross-linked to the zeolite crystals. The results demonstrate that EPR can be a powerful tool for the direct *in situ* analysis of supramolecular photochemistry involving radicals rendered persistent by supramolecular steric effects. The latter eliminate the need for sophisticated flash photolysis equipment to investigate the structure and dynamics of reactive radicals and require only the use of simpler steady-state lamps.

## Introduction

Unless sterically encumbered, carbon-centered radicals in solution are usually transient reactive intermediates possessing a short lifetime (microseconds to milliseconds) as a result of their inherently fast rates of reaction with molecules and other radicals.<sup>1,2</sup> The characterization of the structure and dynamics of reactive radicals in solution requires the use of sophisticated laser flash photolysis equipment with UV, IR, or EPR detection.<sup>3–5</sup> Previously, we have shown that radicals which are very reactive in solution can be rendered 'persistent' (lifetimes of seconds to days) by the application of supramolecular steric effects.<sup>6–9</sup> Ketones, such as dibenzyl ketone (**1a**),<sup>10–12</sup> adsorbed on degassed samples of ZSM-5 zeolites (**1a@ZSM-5**) produce persistent benzyl radicals after photolysis. Under appropriate conditions at room temperature, some of the radicals generated by photolysis are persistent for time periods from seconds to many hours, depending on the supramolecular structure of the radical@zeolite complex and the diffusion and reaction dynamics of the radical. A requirement for persistence of radicals is that the geminate radical pair produced by photolysis must either separate to form free radicals, which must, in turn, diffuse from the external to the internal surface of the zeolite, or, if generated within the internal surface, separate and diffuse apart to form free radicals.<sup>6,7</sup>

Our previous investigations on the EPR of radicals@zeolite complexes were limited to characterization of the radicals

produced by photofragmentation of ketone@zeolite complexes (e.g. Scheme 1, reaction 1) and the kinetic stability of these persistent radicals.<sup>7–9</sup> In this report, we investigate the reactivity of initial persistent benzyl radicals towards acrylate monomers, where persistent adduct radicals are formed by addition of the photogenerated benzyl radicals to the acrylate monomers



**1a** R<sub>1</sub>=R<sub>2</sub>=H

**1b** R<sub>1</sub>=CH<sub>3</sub>, R<sub>2</sub>=H

**1c** R<sub>1</sub>=H, R<sub>2</sub>=CH<sub>3</sub>

**1d** R<sub>1</sub>=H, R<sub>2</sub>=C<sub>2</sub>H<sub>5</sub>

**1e** R<sub>1</sub>=H, R<sub>2</sub>=n-C<sub>5</sub>H<sub>11</sub>

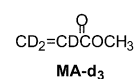
**1f** R<sub>1</sub>=H, R<sub>2</sub>=C<sub>6</sub>H<sub>5</sub>

**3** R<sub>3</sub>=CH<sub>3</sub> (**MA**)

**4** R<sub>3</sub>=C<sub>2</sub>H<sub>5</sub>

**5** R<sub>3</sub>=n-C<sub>5</sub>H<sub>11</sub>

**6** R<sub>3</sub>=n-C<sub>12</sub>H<sub>25</sub>

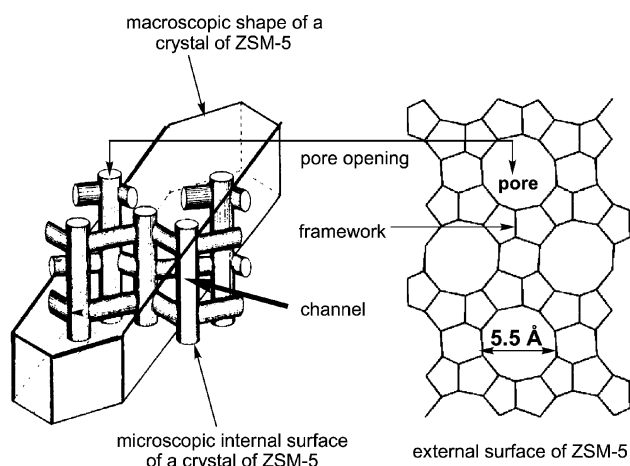


† This paper is dedicated to Professor Fred Lewis on the event of his 60th birthday.

**Scheme 1** Structures of the compounds investigated herein and the photochemistry of dibenzyl ketones.

(Scheme 1, reaction 2). We hypothesized that the steric features of the supramolecular structures of the radical@ZSM-5 species would have a significant effect on the addition rates of the radicals to the acrylates and the lifetimes of the adduct radicals. It was also of interest to find out whether the initial persistent radicals could serve as initiators of the polymerization of acrylates inside the zeolite pores to produce a crosslinked polymer-zeolite material.

The zeolite host selected for this study was ZSM-5 (the Na-exchanged form was examined in this report). The external surface of ZSM-5 crystals consists of pores (circular diameter of the pores *ca.* 5.5 Å) and a solid framework between the pores (Scheme 2). The internal void space consists of channels (*ca.* 5.5 Å in diameter) that intersect to produce roughly spherical supercages of *ca.* 9 Å in diameter.<sup>13,14</sup> As a radical source, we selected a series of dibenzyl ketones (**1**; Scheme 1). The molecular photochemistry of the dibenzyl ketone family of ketones has been well established.<sup>10-12</sup> In common organic solvents after photoexcitation, the initially produced singlet excited state of the dibenzyl ketone is nearly quantitatively transformed to the triplet state and undergoes rapid primary photochemical  $\alpha$  cleavage ( $k_a \approx 10^9 \text{ s}^{-1}$ ), followed by rapid secondary thermal decarbonylation ( $k_{-CO} \approx 10^7 \text{ s}^{-1}$ ) to form free benzyl radicals (**2**).<sup>15-17</sup> Our previous studies showed that the lifetime and mobility of the persistent radicals **2**@ZSM-5 depends on R<sub>2</sub> the alkyl group attached to the  $\alpha$  position of the benzyl radical.<sup>7,8</sup> Therefore, we selected a series of ketones with different R<sub>2</sub> alkyl chain lengths (**1a-e**) as radical precursors



**Scheme 2** Schematic representation of the dimensions of ZSM-5 zeolite.

(Scheme 1) to study the reactivity of these 'initiator' radicals with MA. In addition, a series of *n*-alkyl esters of acrylic acid (**3-6**) were selected to study the reactivity of the different acrylic esters with the persistent benzyl radicals (**2**@ZSM-5) and the properties of the addition products.

## Results and discussion

Photolysis of **1b**@ZSM-5 generates a geminate pair consisting of an *o*-methylbenzyl radical (Scheme 1, R<sub>1</sub> = CH<sub>3</sub>) and **2b**. As we reported previously,<sup>8</sup> the *o*-methylbenzyl radicals and some of the radicals **2b** combine at the external surface (transient radicals). The *o*-methylbenzyl radicals which escape geminate combination are too large to enter the internal surface and, as a result, undergo facile diffusion and combination on the external surface. Therefore, the *o*-methylbenzyl radicals are too short lived to be detected under our EPR conditions and are termed 'transient'. On the other hand, a certain fraction of the radicals **2b** which escape geminate combination diffuse through the pores on the external surface into the internal zeolite surface and become persistent (half-life ~2 min) and are readily detectable under our EPR conditions. Fig. 1(C) shows the EPR spectrum of **2b**@ZSM-5 produced by photolysis of **1b**@ZSM-5. The simulation of the EPR spectrum [Fig. 1(D)] is in good agreement with the assignment. The line shape observed in the spectrum indicates a relatively low mobility for the radical. As expected, no spectral contribution from the *o*-methylbenzyl radical was observed because of its larger size, which prevents its absorption into the internal zeolite surface.

Addition of MA to the zeolite sample containing the persistent radicals (**2b**@ZSM-5) through the gas phase (see Experimental section for details) generated an entirely different EPR spectrum [Fig. 1(E)]. The half-life of this new radical is much longer (many days) than the precursor radical **2b** (~2 min). Benzyl radicals, such as **2b**, are known to add to acrylates, such as methyl acrylate, in solution with a rate constant of  $k = 430 \text{ M}^{-1} \text{ s}^{-1}$ .<sup>1</sup> It is therefore expected that the persistent radical **2b**@ZSM-5 can react with MA to form the adduct radical **7b**@ZSM-5. A simulation of the EPR spectrum of the resulting adduct radical, **7b**@ZSM-5, is shown in Fig. 1(F) and is in good agreement with the assigned structure for the adduct radical [Fig. 1(E)]. Experiments utilizing the deuterated methyl acrylate (MA-d<sub>3</sub>) yielded a different EPR spectrum [Fig. 1(A)], which was assigned to the persistent adduct radical of **2b** to MA-d<sub>3</sub> [**7b**(d<sub>3</sub>)@ZSM-5]; the simulation of this spectrum is shown in Fig. 1(B) and provides further validation of the assignment.

The benzyl radical **2b** can also be generated from dibenzyl ketone, **1a**. However, because of the missing *o*-methyl substiti-

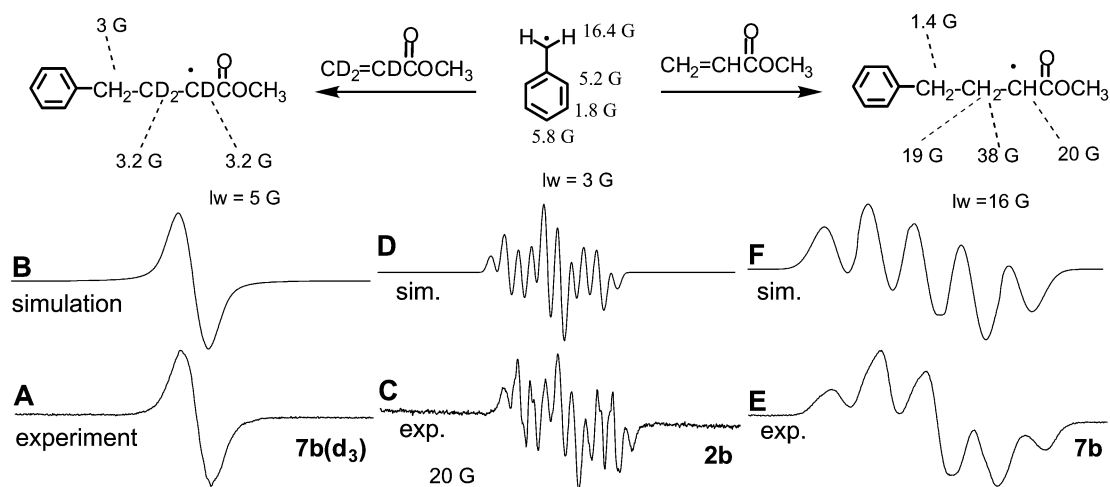


**Fig. 1** EPR spectra of the persistent benzyl radical **2b**@ZSM-5 (generated by photolysis of **1b**@ZSM-5; 1% loading) (C), and the radicals corresponding to the addition product to MA-d<sub>3</sub> [**7b**(d<sub>3</sub>)@ZSM-5] (A) and MA [**7b**@ZSM-5] (E) (1% loading). (D), (B), and (F) are the simulated spectra of (C), (A), and (E), respectively. lw = line width.

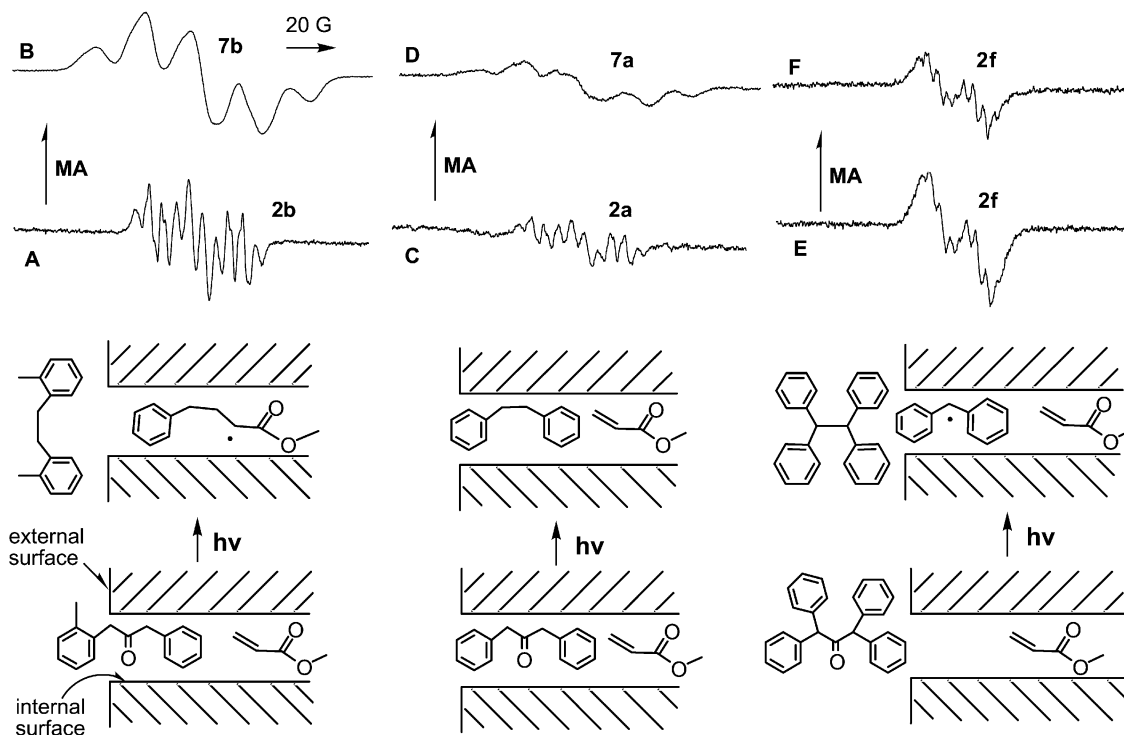


**Fig. 2** EPR spectra of the persistent benzyl radicals **2b** (A) and **2a** (C), and the persistent diphenylmethyl radical (E) on ZSM-5 (generated by photolysis of **1b**, **1a**, and 1,1,3,3-tetraphenylacetone, respectively; 1% loading). EPR spectra of radicals after reaction with MA (3% loading) are shown in (B), (D), and (F), respectively.

tuent in **1a** compared to **1b**, the ketone **1a** is initially absorbed into the internal surface of ZSM-5.<sup>7</sup> Photolysis of **1a** inside the zeolite channels leads, after rapid decarbonylation, to a geminate radical pair of benzyl radicals which are confined to the pores in the internal surface, and this geminate pair may combine or diffuse apart to form persistent free radicals (**2a**@ZSM-5). Because **2b** is generated on or near the external surface (the *o*-methyl group prevents **1a** from entering the internal surface),<sup>7</sup> the *chemically* identical radical **2a** produced from **1a** might have different properties (isomeric supramolecular effects of the zeolite host) with respect to the addition to MA. Fig. 2(C) shows the EPR spectrum of the persistent radical **2a**@ZSM-5, which is identical in terms of line shape to the EPR spectrum of **2b**@ZSM-5 [Fig. 2(A)], but is weaker in intensity. The latter result is probably due to efficient recombination of the geminate radical pair after photocleavage (a relatively efficient cage effect) of **1a** inside the zeolite channels. Addition of MA from the gas phase to the persistent radical **2a**@ZSM-5 generates a persistent adduct radical, **7a**@ZSM-5, with an EPR spectrum [Fig. 2(D)] quite similar to that of **7b**@ZSM-5 [Fig. 2(B)], but with much lower intensity.

Previously, we have shown that photolysis of 1,1,3,3-tetraphenylacetone (**1f**) on ZSM-5 generates very persistent diphenylmethyl radicals (lifetime of several weeks).<sup>9</sup> Fig. 2(E) shows the EPR spectrum of persistent diphenylmethyl radicals on ZSM-5 produced by photolysis of **1f**@ZSM-5. Addition of MA did not cause a noticeable generation of persistent adduct radicals [Fig. 2(F)]. In solution, the addition rate constant of diphenylmethyl radicals to acrylates is relatively low (addition to methyl methacrylate:  $k = 2.5 \text{ M}^{-1} \text{ s}^{-1}$ ).<sup>18</sup> However, because of the long lifetime of **2f**@ZSM-5,<sup>9</sup> significant addition to MA should occur within several hours. Therefore, the low addition rate constant may not be the major cause for the lack of observation of the persistent adduct radical **7f**@ZSM-5. The diameter (molecular cross-section) of the diphenylmethyl radical is approximately the same as the diameter of the zeolite pores of ZSM-5.<sup>9</sup> Therefore, we speculate that the addition of MA to the radical center is probably sterically hindered inside the zeolite, inhibiting adduct radical formation.

Photolysis of ketones **1b** to **1e** adsorbed on ZSM-5 generates persistent radicals **2b** to **2e**, which possess *n*-alkyl chains of different lengths and, therefore, differing supramolecular steric requirements.<sup>7,8</sup> Fig. 3(A) shows a representative example of the EPR spectrum of **2e**@ZSM-5 generated from photolysis of **1e**@ZSM-5. To study the alkyl chain length dependence on the radical initiator, MA-*d*<sub>3</sub> was added to the persistent **2e**@ZSM-5. Directly after addition of MA-*d*<sub>3</sub> through the gas phase to a sample of **2e**@ZSM-5, a new EPR spectrum was observed [Fig. 3(B)]. After 13 h, the EPR spectrum [Fig. 3(C)] changed,

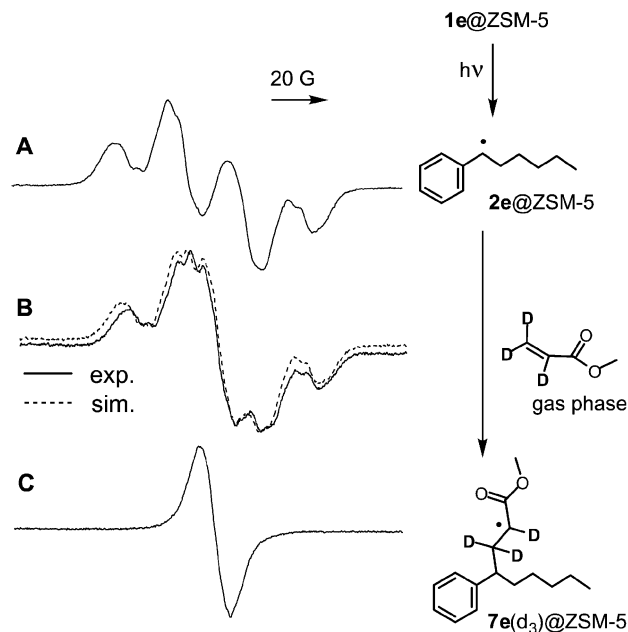


**Fig. 3** EPR spectra of the persistent benzyl radical **2e**@ZSM-5, generated by photolysis of **1e** (1%) on ZSM-5: (A) spectrum of **2e**; (B) spectrum recorded directly after addition of 1% MA-*d*<sub>3</sub> through the gas phase; (C) spectrum after 13 h. The dashed line in B represents the spectrum generated by addition of the spectral components A (57%), and C (43%).

becoming similar to that assigned to the persistent adduct radical shown in Fig. 1(A). Therefore, we assign the EPR signal to the persistent adduct radical  $7e(d_3)$ . The complex EPR spectrum recorded directly after addition of MA [Fig. 3(B), continuous line] is probably the sum of two radicals, the persistent benzyl radical  $2e$  and the adduct radical  $7e(d_3)$ . Addition of the two spectral components using Fig. 3(A) (57%) and Fig. 3(C) (43%) yielded a spectrum [Fig. 3(B), dashed line] which is similar to the experimental spectrum [Fig. 3(B), continuous line]. This indicates that the large radical  $2e$  reacts slowly over several hours with MA- $d_3$ .

In the case of the much smaller persistent benzyl radical  $2b@ZSM-5$ , a much faster reaction with MA added through the gas phase was observed (less than 1 min). The radicals  $2c$  and  $2d$  showed intermediate reactivity with MA. This indicates that the radical reactivity decreases with increasing n-alkyl chain length of the radical moiety of the complex ( $2b \gg 2c > 2d > 2e$ ). Separate experiments with the ketones  $1b-e$  on ZSM-5, in which MA was co-adsorbed on ZSM-5 and the system was photolyzed, yielded similar observations.

The alkyl chain length dependence on the reactivity of the benzyl radical@ZSM-5 complex towards different acryl n-alkyl esters ( $3-6$ ) was next investigated (Scheme 1). The acryl n-alkyl esters  $3-6$  (3%) and  $1b$  (1%) were co-adsorbed on ZSM-5. Irradiation generated the EPR spectra shown in Fig. 4. The strongest signal was observed for MA (ester with the smallest alkyl chain,  $CH_3$ ) and is assigned to the persistent adduct radical  $7b@ZSM-5$ . The shape of the EPR signal remained roughly the same, but the intensity decreased with increasing n-alkyl chain length of the monomer. This result can be ascribed to supramolecular steric factors. With increasing chain length, the diffusion of the acrylates through the zeolite channels is hindered and, therefore, the scavenging of the persistent benzyl radicals ( $2b$ ) by the acrylates is reduced. In addition, the rate of addition of the benzyl radical to an acrylate, once the radical encounters a monomer, may decrease as the size of the alkyl chain on the ester increases, due to supramolecular steric effects.

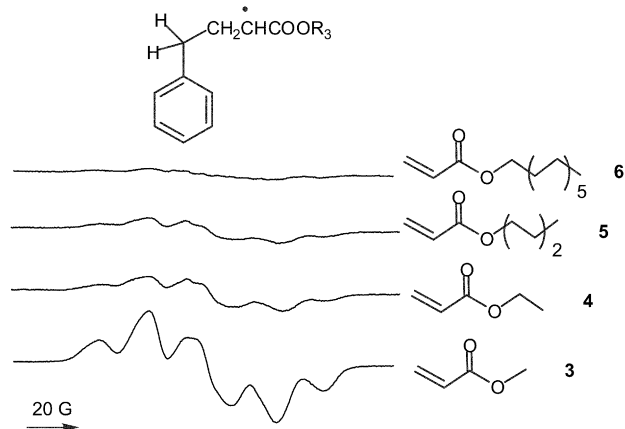


**Fig. 4** EPR spectra of the addition product of  $2b$  [generated by photolysis of  $1b$  (1%) on ZSM-5] to different n-alkyl acryl esters,  $3-6$  (3%).

In order to investigate whether the decay kinetics of the persistent adduct radical  $7@ZSM-5$  was dependent on the concentration of the acrylate monomer, we followed the EPR signal intensity of  $7b@ZSM-5$  over time at different concentrations of MA as monomer (Fig. 5). The precursor radical  $2b@ZSM-5$  has a half-life of approximately 2 min. Fig. 5 indicates that the half-life of the adduct radical increases dramatically with increasing loading of MA. At 0.4% loading of MA, the adduct radical  $7b$  shows a half-life of approximately 80 h, while an almost infinite radical half-life is observed at 10% loading of MA. Over time, small changes in the peak positions of the EPR spectra occurred, indicating a change in the radical structure. These are

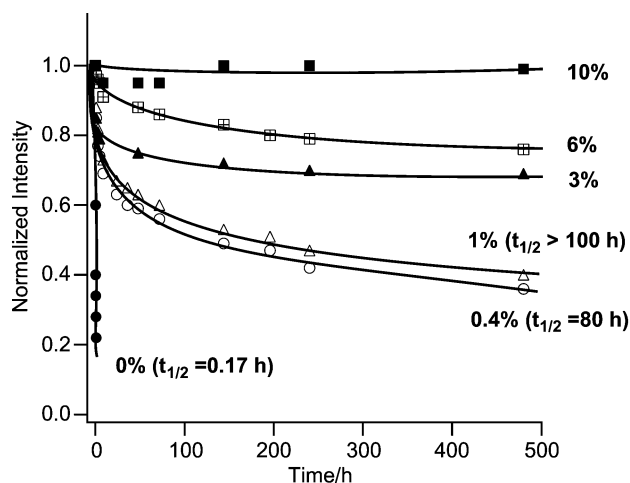


**Fig. 5** Normalized EPR intensity (corresponding to persistent adduct radical) vs. time after addition of different concentrations of MA to persistent  $2b@ZSM-5$  (generated by photolysis of  $1b@ZSM-5$ ).

probably attributable to propagating radicals, where the adduct radical  $7b$  adds to MA to generate a secondary adduct radical,  $8b$ , and so on. The lifetime of the propagating radical is longer at high loadings of MA than at low MA loadings, probably because propagation is favored over competing termination at high loadings. At low loadings of MA, radical termination reactions can compete with the propagation.

To demonstrate that propagation and polymerization of MA initiated by  $2@ZSM-5$  had occurred, the monomers MA- $d_3$  and MA were added subsequently. Fig. 6 shows an example. Photolysis of  $1b@ZSM-5$  yielded the persistent radical  $2b@ZSM-5$  (spectrum A). After reaction with MA- $d_3$  the deuterated adduct radical  $7b(d_3)@ZSM-5$  is formed (spectrum B). The latter is in good agreement with the simulated spectrum [Fig. 1(B)]. Because of the deuteration, the EPR spectrum is easily distinguishable from the adduct radical using MA. Subsequent addition of MA to the persistent deuterated adduct radical  $7b(d_3)@ZSM-5$  yielded the spectrum plotted with a continuous line in Fig. 6(C), which shows the  $^1H$ -hyperfine coupling of the addition product to MA. Simulation (dashed line) of the experimental spectrum (continuous line) [Fig. 6(C)] shows that addition to MA occurred to 59%. Spectrum C indicates that the sample still contains a significant amount of the adduct radical to MA- $d_3$  (41%). This could be attributed to radicals trapped in zeolite locations where MA cannot diffuse to, or to secondary adducts formed with the remaining MA- $d_3$ . Additional experiments were performed, where the acrylate addition sequence was reversed. Non-deuterated MA was added to persistent benzyl radical  $2b@ZSM-5$  to form the adduct radical  $7b@ZSM-5$ . Subsequent addition of MA- $d_3$  yielded a narrow EPR spectrum similar to Fig. 6(B).

To test whether polymerization of MA occurred through initiation by persistent benzyl radicals on ZSM-5,  $1b$  (1%) adsorbed on ZSM-5 was photolyzed and exposed to MA vapor under reduced pressure at room temperature for one month. A semi-transparent rubber-like polymer was formed on the zeolite, which did not dissolve in methylene chloride or THF. The polymer formed by free radical polymerization of MA in solution consists of linear polymer chains, which are readily soluble in THF. Because the polymer produced by polymerization on ZSM-5 is insoluble in THF, we propose that the linear polymer chains are cross-linked by the zeolite crystals. The growing polymer chains could extend from the zeolite surface, and polymer radicals on two different zeolite crystals could recombine and cross-link the zeolite.

## Conclusions

Photolysis of the supramolecular complexes of dibenzyl ketones on ZSM-5 ( $1@ZSM-5$ ) produces persistent benzyl

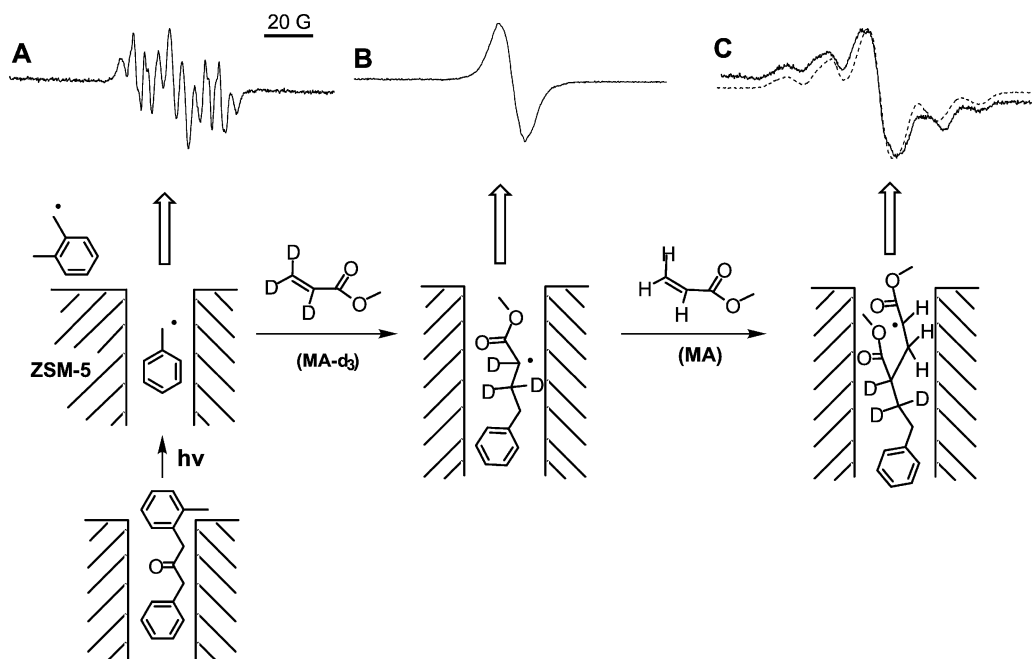


**Fig. 6** EPR spectra of radical intermediates during MA polymerization initiated by **2b**@ZSM-5, generated by photolysis of **1b** on ZSM-5: (A) spectrum of **2b**; (B) spectrum of the adduct to MA- $d_3$ ; (C) spectrum of the subsequent adduct to MA (continuous line). The dashed line in C represents the spectrum generated by addition of the spectral components of the adduct radical of **2b**@ZSM-5 with MA and MA- $d_3$ .

radicals (**2**@ZSM-5), which add to methyl acrylate (MA) to form persistent adduct radicals (**7**@ZSM-5). The rate of formation and the amount of the persistent adduct radical depends on the structure of the initiator (benzyl radical). The highest EPR signal intensity and highest addition rate to MA was observed for the smallest initiator radical (**2b**), probably because of its high mobility and ability to diffuse throughout the zeolite internal surface. As the length of the alkyl chain was increased (**2c–e**) the rate of the radical addition to MA decreased, which is consistent with the decreased mobility of the primary radical. The diphenylmethyl radical did not show a detectable reaction with MA, probably because of the steric hinderance it experiences inside the zeolite pores. As further evidence of the role of supramolecular steric factors, decreasing the mobility of the acrylates by using *n*-alkyl esters of different chain length (**3–6**) yielded lower amounts of the persistent adduct radical (**7**@ZSM-5).

Deuterium isotope experiments and variation of MA concentration showed that the adduct radical (**7**@ZSM-5) adds to MA to generate a secondary adduct radical, **8**@ZSM-5, which, in turn, can continue to propagate to form a polymer cross-linking the zeolite crystals.

## Experimental

### Materials

All chemicals, unless noted otherwise, were obtained from Aldrich and used as received. Sodium-exchanged ZSM-5 (Si/Al = 20) was a generous gift from CU Chemie Uetikon AG, Uetikon, Switzerland. The mean crystal diameter was 0.5  $\mu\text{m}$ , as characterized by scanning electron microscopy. The external surface area was determined by EPR spectroscopy (spin probe: 2,2,6,6-tetramethyl-4-[(phenylacetyl)oxy]-1-piperidinyloxy)<sup>19</sup> to be 20  $\text{m}^2 \text{g}^{-1}$ .

1,3-Diphenyl-2-propanone (**1a**) from Aldrich was purified by re-crystallization from 5% (v/v) diethyl ether in hexane. 1-(2-methylphenyl)-3-phenyl-2-propanone (**1b**), 2,4-diphenyl-pentan-3-one (**1c**), 3,5-diphenyl-heptan-4-one (**1d**), and 6,8-diphenyl-tridecan-7-one (**1e**) were synthesized following the procedure described previously.<sup>7</sup> Methyl acrylate- $d_3$  (MA- $d_3$ ) was synthesized from acrylic- $d_3$  acid- $d$ .<sup>20</sup> acrylic- $d_3$  acid- $d$  (1 g, 0.0132 mol), *N,N*-dicyclohexylcarbodiimide (3.15 g, 0.0153 mol),

methanol (0.5 g, 0.0154 mol), and 4-pyrrolidinopyridine (0.21 g, 0.0014 mol) in 25 mL of isooctane were stirred in a 50 mL round-bottom flask at room temperature (5 h) until esterification was nearly completed (95% conversion, by GC). The *N,N*-dicyclohexyl urea was filtered out and the filtrate was distilled under reduced pressure. <sup>1</sup>H-NMR gave only a single peak at 3.766 ppm due to methyl acrylate- $d_3$ .

### Sample preparation

ZSM-5 zeolite was activated in a furnace at 500 °C for approximately 2 h and cooled in a desiccator to room temperature before use. A typical sample preparation procedure was as follows. The loading of the ketone, acrylate, or a mixture of ketone and acrylate was achieved by stirring a weighed amount of the ketone and/or acrylate in a solution of 0.3 mL of isooctane with 100 mg of ZSM-5 zeolite in a vial for 1 h. After evaporation of the solvent under flowing argon, the samples were transferred into a branched quartz cell and degassed under vacuum to  $2 \times 10^{-5}$  Torr. For step-by-step addition experiments, a cell with a branch for EPR measurement and an acrylate container was designed,<sup>21</sup> with which the zeolite sample and acrylates can be degassed and sealed separately. For example, a sample of the ketone already loaded on ZSM-5 was placed in the cell and sealed by closing the valve, while methyl acrylate was placed into the acrylate branch of the cell, degassed by 3 freeze–pump–thaw cycles, and sealed with a valve. Afterwards, the branch of the cell containing the zeolite sample was degassed by pumping to  $2 \times 10^{-5}$  Torr and sealed by closing the valve again.

### Photolysis

The degassed samples of the ketone (or the ketone with the acrylate) adsorbed on the zeolite were irradiated in the quartz cell for 8 min using a 450 W medium pressure mercury lamp (Hanovia) equipped with a chromate filter solution or a glass filter which cut the wavelength below 290 nm. In order to ensure homogeneous irradiation of the zeolite powder, the cell was rotated in front of the lamp. Immediately after photolysis, the sample was transferred into the 3 mm quartz tube of the branched cell for EPR analysis. For step by step addition experiments, MA (or MA- $d_3$ ) was added through the gas phase by opening the acrylate container on the cell.<sup>21</sup>

## EPR measurements

The EPR measurements were performed at room temperature using a Bruker EMX spectrometer operating at X-band (9.5 GHz).

## Simulation of EPR spectra

Computer simulations of the EPR spectra were performed by means of the Simfonia program (Bruker), considering a powder spectrum in which the anisotropies are averaged. Often, a large line width was necessary to reproduce the experimental line shape. This line broadening includes the small hyperfine couplings of distant protons or deuterium atoms, but also includes partially hindered rotation of the radicals. The simulation of the EPR spectra of benzyl radicals (**2**) and the adduct radicals to methyl acrylate (**7**) were based on the proton–electron hyperfine coupling constants reported in the literature.<sup>22</sup> The deuterium–electron hyperfine coupling constants for the acrylate additive radicals were assumed to be *ca.* one sixth of those of their proton counterparts.

## Acknowledgements

The authors at Columbia University thank the National Science Foundation for its generous support of this research through grant CHE-01-10655; this work was also supported in part by the MRSEC program of the National Science Foundation under award no. DMR-02-13574. M. F. O. thanks the Italian Ministero dell'Università e della Ricerca Scientifica (MURST) and COFIN2000 for financial support. The authors also thank the National Science Foundation for a travel grant (INT-00-91547).

## References

- 1 H. Fischer and L. Radom, Factors controlling the addition of carbon-centered radicals to alkenes - an experimental, and theoretical perspective, *Angew. Chem., Int. Ed.*, 2001, **40**, 1340–1371.
- 2 D. Griller and K. U. Ingold, Persistent carbon-centered radicals, *Acc. Chem. Res.*, 1976, **9**, 13–19.
- 3 J. C. Scaiano, *Handbook of Organic Photochemistry*; CRC Press, Boca Raton, 1989, vol. 1.
- 4 J. J. Turner, M. W. George and M. Poliakoff, *Recent Advances in Kinetic Infrared Spectroscopy*, Spec. Publ. - R. Soc. Chem., Royal Society of Chemistry, Cambridge, 1995.
- 5 M. D. E. Forbes, Time-resolved (CW) electron paramagnetic resonance spectroscopy: an overview of the technique, and its use

- in organic photochemistry, *Photochem. Photobiol.*, 1997, **65**, 73–81.
- 6 N. J. Turro, From boiling stone to smart crystals: supramolecular, and magnetic isotope control of radical-radical reactions in zeolites, *Acc. Chem. Res.*, 2000, **33**, 637–646.
- 7 N. J. Turro, X.-G. Lei, S. Jockusch, W. Li, Z. Liu, L. Abrams and M. F. Ottaviani, EPR investigation of persistent radicals produced from the photolysis of dibenzyl ketones adsorbed on ZSM-5 zeolites, *J. Org. Chem.*, 2002, **67**, 2606–2618.
- 8 N. J. Turro, S. Jockusch and X.-G. Lei, Supramolecular effects on the dynamics of radicals in MFI zeolites: a direct EPR investigation, *J. Org. Chem.*, 2002, **67**, 5779–5782.
- 9 T. Hirano, W. Li, L. Abrams, P. L. Krusic, M. F. Ottaviani and N. J. Turro, Supramolecular steric effects as the means of making reactive carbon radicals persistent. Quantitative characterization of the external surface of MFI zeolites through a persistent radical probe, and a Langmuir adsorption isotherm, *J. Org. Chem.*, 1999, **65**, 1319–1330.
- 10 P. S. Engel, Photochemistry of dibenzyl ketone, *J. Am. Chem. Soc.*, 1970, **92**, 6074–6076.
- 11 W. K. Robbins and R. H. Eastman, Photodecarbonylation in solution. I. Quantum yields, and quenching results with dibenzyl ketones, *J. Am. Chem. Soc.*, 1970, **92**, 6076–6077.
- 12 W. K. Robbins and R. H. Eastman, Photodecarbonylation in Solution. II. Trapping of intermediates in the photolysis of dibenzyl ketone, *J. Am. Chem. Soc.*, 1970, **92**, 6077–6079.
- 13 W. M. Meier and D. H. Olson, *Atlas of Zeolite Structure Types*, Butterworth-Heinemann, London, 1992.
- 14 M. E. Davis and R. F. Lobo, Zeolite, and molecular sieve synthesis, *Chem. Mater.*, 1992, **4**, 756–768.
- 15 I. R. Gould, B. H. Baretz and N. J. Turro, Primary processes in type I photocleavage of dibenzyl ketones. A pulsed laser, and photochemically induced dynamic nuclear polarization study, *J. Phys. Chem.*, 1987, **91**, 925–929.
- 16 C. Arbour and G. H. Atkinson, Picosecond photodissociation of dibenzyl ketone, *Chem. Phys. Lett.*, 1989, **159**, 520–525.
- 17 L. Lunazzi, K. U. Ingold and J. C. Scaiano, Absolute rate constants for the decarbonylation of the phenylacetyl radical, *J. Phys. Chem.*, 1983, **87**, 529–530.
- 18 K. Ito, M. Omi and T. Ito, Kinetics of radical polymerization with primary radical termination, *Polym. J.*, 1982, **14**, 115–120.
- 19 M. F. Ottaviani, X.-G. Lei, Z. Liu and N. J. Turro, Supramolecular structure, and dynamics of organic molecules adsorbed on the external surface of MFI zeolites. A direct, and indirect computational EPR analysis, *J. Phys. Chem. B*, 2001, **105**, 7954–7962.
- 20 A. Hassner and V. Alexanian, Direct room temperature esterification of carboxylic acids, *Tetrahedron Lett.*, 1978, **19**, 4475–4478.
- 21 T. L. Morkin, N. J. Turro, W. H. Kramer and I. R. Gould, A novel selective solid state photooxidant, *J. Am. Chem. Soc.*, submitted.
- 22 M. S. Conradi, H. Zeldes and R. Livingston, ESR and Ring inversion of tetralin-1-yl and ESR of related benzyl radicals, *J. Phys. Chem.*, 1979, **83**, 633–637.